ARTICLE
Journal of Cellular Biochemistry 112:2019–2029 (2011)

Journal of Cellular Biochemistry

Protective Effects of Cynaroside Against H_2O_2-Induced Apoptosis in H9c2 Cardiomyoblasts

Xiao Sun, Gui-bo Sun, Min Wang, Jing Xiao, and Xiao-bo Sun*

Institute of Medicinal Plant Development (IMPLAD), Chinese Academy of Medical Sciences & Peking Union Medical College, No. 151, Malianwa North Road, HaiDian District, Beijing 100193, PR China

ABSTRACT

Flavonoids with potent anti-oxidative effects are the major effective components in traditional herbal medicine used in treating cardiovascular diseases. Cynaroside is a flavonoid compound that exhibits anti-oxidative capabilities. However, little is known about its effect on oxidative injury to cardiac myocytes and the underlying mechanisms. This study was designed to investigate the protective effects of cynaroside against H_2O_2-induced apoptosis in H9c2 cardiomyoblasts. H9c2 cells were pretreated with cynaroside for 4 h before exposure to 150 μM H_2O_2 for 6 h. H_2O_2 treatment caused severe injury to the H9c2 cells, which was accompanied by apoptosis, as revealed by analysis of cell nuclear morphology, through Annexin V FITC/PI staining and caspase proteases activation. Cynaroside pretreatment significantly reduced the apoptotic rate by enhancing the endogenous anti-oxidative activity of superoxide dismutase, glutathione peroxidase, and catalase, thereby inhibiting intracellular reactive oxygen species (ROS) generation. Moreover, cynaroside moderated H_2O_2-induced disruption of mitochondrial membrane potential, increased the expression of anti-apoptotic protein Bcl-2 while decreased the expression of pro-apoptotic protein Bax, and thereby inhibited the release of apoptogenic factors (cytochrome *c* and smac/Diablo) from mitochondria in H9c2 cells. Our data also demonstrated that cynaroside pretreatment showed an inhibitory effect on the H_2O_2-induced increase in c-Jun N-terminal kinase (JNK) and P53 protein expression. These results suggest that cynaroside prevents H_2O_2-induced apoptosis in H9c2 cell by reducing the endogenous production of ROS, maintaining mitochondrial function, and modulating the JNK and P53 pathways. J. Cell. Biochem. 112: 2019–2029, 2011.

KEY WORDS: CYNAROSIDE; OXIDATIVE STRESS; APOPTOSIS; MITOCHONDRIAL DYSFUNCTION

Cardiovascular disease is one of the most prevalent diseases in both developed and developing countries, with high morbidity and high risk of death [Smith, 2000; Khor, 2001]. Cardiac myocyte apoptosis, which causes massive cell loss and eventually affects the long-term prognosis, is involved in the pathogenesis of various cardiovascular diseases such as myocardial infarction, ischemia/reperfusion injury, and heart failure. It has always been a major focus of medical research [Gottlieb et al., 1994; Kang and Izumo, 2000; Kim and Kang, 2010].

Oxidative stress, intracellular Ca^{2+} overload, and mitochondrial dysfunction are the common stressors that induce cardiomyocyte apoptosis, among which oxidative stress has gained much attention. Oxidative stress is usually defined as the non-homeostatic states wherein production of partially reduced forms of O_2, referred to as reactive oxygen species (ROS), exceed cellular detoxification or utilization [Pryor et al., 2006]. Abnormal accumulation of intracellular ROS may cause detrimental modification of important cellular macromolecules. Lipid peroxidation leads to structural and functional changes in cellular membrane. The sulfhydryl and amino oxidation of proteins might cause the loss of enzymatic activity. DNA damage triggers cell mutation [Ryter et al., 2007]. These cumulative damages may ultimately evoke apoptosis through different pathways. Hence, regulation of intracellular ROS and modification of the apoptotic cascade may be an effective way to reduce pathological apoptosis. Flavonoids, a group of polyphenol compounds, constitute a major part of effective components in

Xiao Sun and Gui-bo Sun contributed equally to this work.

Grant sponsor: Key Projects in the National Science & Technology Pillar Program; Grant number: 2008BAI51B02; Grant sponsor: Major Scientific and Technological Special Project for "Significant New Drugs Formulation "; Grant number: 2009ZX09301-003.

*Correspondence to: Xiao-bo Sun, Institute of Medicinal Plant Development (IMPLAD), Chinese Academy of Medical Sciences & Peking Union Medical College, No. 151, Malianwa North Road, HaiDian District, Beijing 100193, PR China. E-mail: sunxiaobosubmit@163.com

Received 22 October 2010; Accepted 17 March 2011 • DOI 10.1002/jcb.23121 • © 2011 Wiley-Liss, Inc.
Published online 28 March 2011 in Wiley Online Library (wileyonlinelibrary.com).

traditional Chinese herbal medicines, such as *Ginkgo biloba*, *Panax notoginseng*, and Radix Puerariae and so on, that are frequently used to treat cardiovascular disease [Mahady, 2002; Ng, 2006; Zhang et al., 2008; Mojzisova et al., 2009]. They demonstrate diverse biological and pharmacological effects, including anti-inflammatory, vasodilatation, and improving blood circulation, among others. However, they are well known for their potent anti-oxidative ability, which contributes most to their cardiovascular protective effects. For example, the leaf extracts of *G. biloba* has been widely known for its anti-oxidant capacities and is used to treat dementia and cardiovascular diseases worldwide. *G. biloba* leaf extract contains 24–27% flavonoids, which are its major effective components and are responsible for its anti-oxidant activity [Mahady, 2002; Zhou et al., 2004; Bent, 2008].

Cynaroside is luteolin-7-*O*-glucoside, one of the flavonoid compounds found in many medicinal plants (Fig. 1), and in vitro experiments have shown that it scavenges oxygen free radicals and reduces low-density lipoprotein oxidation [Brown and Rice-Evans, 1998; Wu et al., 2005]. An earlier study [Rump et al., 1994] reported that cynaroside showed anti-ischemic effects in isolated rat hearts, which might be related to its anti-oxidative properties. Therefore, investigating the potential of cynaroside for preventing oxidative stress-induced cardiomyocyte apoptosis has attracted our attention. Quercetin, one of the well-studied flavonoids with potent protective effects against oxidative stress-induced cardiac myocyte apoptosis, served as the positive control in this study [Park et al., 2003; Han et al., 2008].

In this study, the effects of cynaroside on H9c2 cardiomyoblasts apoptosis induced by H_2O_2 were investigated. H_2O_2 has been extensively used as an inducer of oxidative stress in vitro [Ryter et al., 2007]. The H9c2 cell line, derived from embryonic BDIX rat heart tissue expressing specific cardiac markers, is considered a close surrogate for cardiomyocytes and widely used in studies investigating cardiomyocyte cellular mechanisms [Kimes and Brandt, 1976; Hescheler et al., 1991; Wu et al., 1996]. The possible mechanisms of cynaroside protection were also studied by measuring intracellular ROS, the mitochondrial membrane potential, and the expression of apoptosis-related proteins Bcl-2, Bax, c-Jun N-terminal kinase (JNK) and P53.

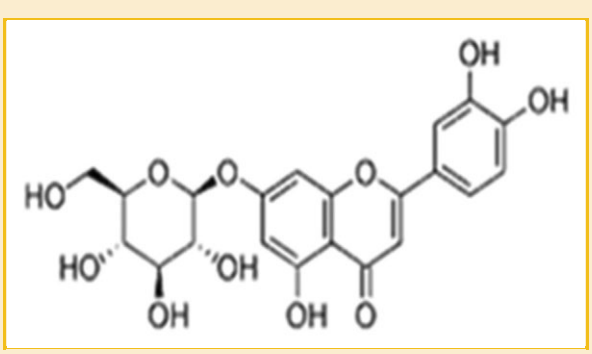

Fig. 1. Molecular structure of cynaroside.

MATERIALS AND METHODS

CHEMICALS AND MATERIALS

Cynaroside and quercetin (purity >99%) were obtained from Shanghai Winherb Medical S & T Development (Shanghai, China). H_2O_2 was purchased from Beijing Chemical Works (Beijing, China). Cell culture products were purchased from Gibco BRL (Grand island, NY). Fluorescent dyes Hoechst 33342 and JC-1 were purchased from Sigma-Aldrich (St. Louis, MI). The kits for determining lactate dehydrogenase (LDH) and malondialdehyde (MDA) contents and superoxide dismutase (SOD), catalase (CAT), glutathione peroxidase (GSH-Px) activity were obtained from Jiancheng Bioengineering Institute (Nanjing, China). Annexin V/fluorescein isothiocyanate/propidium iodide (FITC/PI) apoptosis kit was obtained from Invitrogen (Eugene, OR). Caspase-3, -8, and -9 Fluorometric Assay Kits were acquired from BioVision (Palo Alto, CA). Primary antibodies against Bcl-2, Bax, apoptotic protease-activating factor 1 (Apaf-1), cytochrome *c*, Smac/Diablo, JNK, p-JNK, and P53 were from Santa Cruz Biotechnology (CA). β-actin, GAPDH primary antibodies, and horseradish peroxidase (HRP)-conjugated secondary antibodies were from CWbiotech (Beijing, China). The purity of all chemical reagents was at least of analytical grade.

CELL CULTURE

Rat embryonic cardiomyoblast-derived H9c2 cells were obtained from the Cell Bank of the Chinese Academy of Sciences (Shanghai). The cells were cultured in Dulbecco's modified Eagle's medium supplemented with 10% (v/v) fetal bovine serum, 2 mM L-glutamine, 100 U/ml of penicillin, 100 μg/ml of streptomycin and maintained in a humidified incubator of 95% air/5% CO_2 at 37°C [Park et al., 2003]. Cells in the exponential phase of growth were used. For all experiments, the cells were plated at an appropriate density according to the experimental design and were grown for 36 h before experimentation.

ANALYSIS OF CELL VIABILITY AND MORPHOLOGICAL CHANGES

Cell viability was determined colorimetrically by 3-(4,5-dimethylthiazol-2-yl)-2,5-diphenyl tetrazolium (MTT) assay. Briefly, cells were seeded at 1×10^4 cells/well in 96-well plates. After 4 h of treatment with different concentrations of cynaroside followed by incubation with 150 μM H_2O_2 for 6 h, 20 μl of 5 mg/ml MTT solution was added to each well (0.1 mg/well), and incubated for 4 h. The supernates were aspirated, and the formazan crystals in each well were dissolved in 100 μl of DMSO. The absorbance was measured at 570 nm on a microplate reader (BioTek, Vermont). The morphological changes in the cells were also observed and the images were captured under an inverted microscope connected to a digital camera (Canon Inc., Tokyo, Japan).

MEASUREMENT OF LDH AND MDA LEVELS AND THE ACTIVITY OF SOD, CAT, AND GSH-Px

The H9c2 cells were cultured in 6-well plates at 3×10^5 cells/well. The supernate and the cells were collected, respectively, after the different treatments for measuring the LDH and MDA levels, as well as SOD, CAT, and GSH-Px activity with the corresponding detection kit according to the manufacturer's instructions [Han et al., 2008].

MORPHOLOGICAL ASSESSMENT AND QUANTIFICATION OF APOPTOTIC MYOCYTES

Hoechst 33342 staining, which distinguishes apoptotic from normal cells based on nuclear chromatin condensation and fragmentation, was used for the qualitative and quantitative analyses of the apoptotic myocytes. The H9c2 cells were cultured on cover slips in 6-well plates for 36 h. After treatment, the cells were incubated with 5 μg/ml Hoechst 33342 for 15 min, washed twice with phosphate-buffered saline (PBS), and visualized by fluorescence microscopy (Leica, Heidelberg, Germany) [Fu et al., 2007]. The apoptotic nuclei were counted in at least 200 cells from five randomly selected fields in each treatment, and expressed as a percentage of the total number of nuclei counted.

FLOW CYTOMETRIC DETECTION OF APOPTOSIS

Early apoptosis and necrosis were identified by double fluorescence staining using the Annexin V-FITC/PI Apoptosis kit according to the manufacturer's brochures (Invitrogen). The phosphatidylserine in the apoptotic cells translocated from the inner plasma membrane to the outer surface while the membrane remained physically intact, whereas Annexin V-FITC binds with high affinity to phosphatidylserine. PI entered the cells when the membranes were disrupted or the permeability increased during necrosis or at the late stage of apoptosis. The cells were harvested, washed twice with cold PBS, incubated with the 5 μl FITC-Annexin V and 1 μl PI working solution (100 μg/ml) for 15 min in the dark at room temperature, and then cellular fluorescence was measured by flow cytometry analysis with a FACSCalibur Flow Cytometer (BD Biosciences, Franklin Lakes, NJ).

DETECTION OF INTRACELLULAR ROS PRODUCTION

To investigate the effect of cynaroside on the generation of intracellular ROS, the cells were pretreated with cynaroside for 4 h prior to the addition of 150 μM H_2O_2 for 6 h. Then, the level of intracellular ROS was monitored using the total ROS detection kit according to the manufacturer's brochures (Enzo life sciences, Farmingdale, NY). The cells were harvested, placed into 5 ml round-bottom polystyrene tubes after treatment, and washed with 1× wash buffer. Then, the cells were centrifuged for 5 min at 400*g* at room temperature and the supernate was discarded. The cells were resuspended in 500 μl ROS detection solution, stained at 37°C in the dark for 30 min, and then analyzed by flow cytometry.

DETERMINATION OF MITOCHONDRIAL TRANSMEMBRANE POTENTIAL ($\Delta\Psi_m$)

5,5′,6,6′-Tetrachloro-1,1′,3,3′-tetraethylbenzimidazolyl-carbocyanine iodide (JC-1) (Invitrogen) was used to determine the changes in mitochondrial transmembrane potential. JC-1 exhibits potential-dependent accumulation in mitochondria. In normal healthy cells, JC-1 accumulates and forms dimeric J-aggregates in the mitochondria, giving off a bright red fluorescence. However, when the potential is disturbed, the dye cannot access the transmembrane space and remains in the cytoplasm in its monomer form (green fluorescence). Consequently, mitochondrial depolarization is indicated by an increase in the green/red fluorescence intensity ratio, which may determine the percentage of mitochondria within a population that respond to the applied stimulus. After thorough removal of H_2O_2, the cells were suspended in warm medium at approximately 1×10^6 cells/ml. Then, 10 μl of 200 μM JC-1 (2 μM final concentration) was added and the cells were incubated for 30 min in the dark, and then washed twice with PBS [Shan et al., 2008]. The cells labeled with JC-1 were analyzed by flow cytometry using 488 nm excitation and green or orange-red emission wavelengths.

ANALYSIS OF CASPASE-3 ACTIVATION AND CASPASE-8 AND CASPASE-9 ACTIVITY

Caspase-3 activation was measured using a fluorescein active caspase-3 staining kit (BioVision). About 300 μl (1×10^6 cells/ml) of the cultures were incubated with 1 μl substrate FITC-DEVD-FMK for 1 h at 37°C. The cells were centrifuged at 3,000 rpm for 5 min and the supernate was removed, then the cells were washed twice with PBS, resuspended in 300 μl of wash buffer, and kept on ice. The samples were analyzed by flow cytometry using the FL-1 channel. Caspase-8 and caspase-9 activity were measured using a Fluorometric Assay Kit (BioVision) according to the manufacturer's instructions. The cells were resuspended in lysis buffer and kept on ice for 10 min. Then, 50 μl of 2× reaction buffer containing 10 mM dithiothreitol was added to each sample with 5 μl of 1 mM substrate (IETD-AFC or LEHD-AFC for caspase-8 or caspase-9, respectively) was added, and specimens were incubated at 37°C for 1.5 h. The samples were read in a Fluoroskan Ascent FL fluorometer (Thermo Fisher Scientific, MA) at 400 nm excitation and 505 nm emission wavelengths. The fold-increases in caspase activity were determined by comparing the results with the level of the uninduced control.

WESTERN BLOT ANALYSIS

Cultured H9c2 cells were harvested, washed with PBS, and lysed with cell lysis buffer containing 1% phenylmethylsulfonylfluoride. The lysate was centrifuged at 12,000*g* and 4°C for 15 min to remove the insoluble materials. Supernates were collected. For cytochrome *c* and smac, the mitochondrial and cytosolic fractions were separated by Cell Mitochondrial Isolation Kit (Beyotime, Haimen, China) according to the manufacturer's instructions. The protein concentration was measured by bicinchoninic acid assay. Equal amounts of protein (20 μg) from each sample was separated by 12% SDS–PAGE and transferred onto a nitrocellulose membrane (Millipore Corporation, Bedford, MD). Non-specific sites were blocked by the incubating membranes (2 h, room temperature) in 5% (w/v) non-fat milk powder in Tris-buffered saline containing 0.05% (v/v) Tween-20 (TBS-T). Then, the membranes were incubated overnight at 4°C with the primary antibodies from Santa Cruz Biotechnology (Bcl-2, 1:200; Bax, 1:250; Apaf-1, 1:200; cytochrome *c*, 1:200; Smac/Diablo, 1:200; JNK, 1:1,000; p-JNK, 1:400; P53, 1:400). The membranes were washed with TBS-T and incubated with the appropriate secondary HRP-conjugated antibodies at a 1:4,000 dilution. Following a 30 min wash, the membranes were visualized by enhanced chemiluminescence. The band intensity was measured and quantified.

STATISTICAL ANALYSIS

All data are expressed as means ± SD from at least three independent experiments. The differences were analyzed by

ANOVA, followed by post hoc analysis with Student–Newman–Keuls test. Statistical significance was considered at $P < 0.05$.

RESULTS

CYNAROSIDE AMELIORATED H_2O_2-INDUCED CYTOTOXICITY IN H9c2 CELLS

The H9c2 cells were exposed to H_2O_2 at different concentrations (0–800 μM) for 6 h and cell viability was assessed via an MTT assay. H_2O_2 exhibited cytotoxicity in a dose-dependent manner. As shown in Figure 2A, the decrease in cell viability was statistically significant at 50 μM H_2O_2, whereas cell viability was reduced to 46.5% at 150 μM H_2O_2. High concentrations of H_2O_2 caused severe cell damage, and the cell viability was only 1.2% and 0.7% at 400 and 800 μM, respectively. A previous study reported that relatively low concentrations of H_2O_2 caused apoptotic death of more cells (maximal at 250 μM), whereas 1,000 μM H_2O_2 resulted in a reduction in apoptosis but an increase in overall cell death [Turner et al., 1998]. Therefore, in our system, 150 μM H_2O_2 was used in the subsequent experiments. Pretreatment with cynaroside protected the cells from H_2O_2-induced cytotoxicity in a dose-dependent manner. As shown in Figure 2B, cell viability declined to 51.9 ± 7.1% after exposure to 150 μM H_2O_2 for 6 h, whereas it increased to 74.2 ± 5.3% and 93.7 ± 4.0% with 50 and 100 μg/ml cynaroside, respectively. The 25 μg/ml cynaroside pretreatment showed no significant effect on the H_2O_2-induced cytotoxicity.

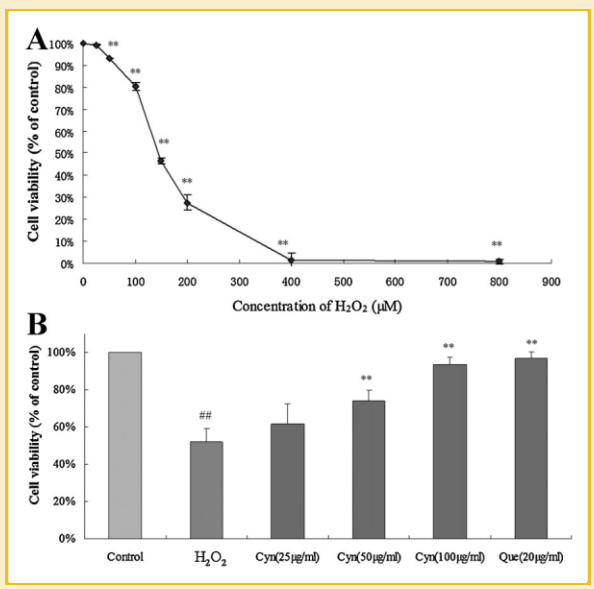

Fig. 2. Protective effects of cynaroside against H_2O_2-induced H9c2 cell injury. A: Effects of H_2O_2 on H9c2 cell viability. The cells were treated with increasing concentrations of H_2O_2 (0–800 μM) for 6 h. Cell viability was measured by MTT assay. B: Effects of cynaroside on H_2O_2-induced H9c2 cell injury. H9c2 cells were pretreated with different concentrations of cynaroside or quercetin for 4 h before 150 μM H_2O_2 was added into the medium. After incubation for 6 h at 37°C, cell viability was determined by MTT assay (A and B, expressed as the percentage of control). Cyn, cynaroside; Que, quercetin. The data are expressed as means ± SD from three independent experiments. $^{\#\#}P < 0.01$ versus control; $^{**}P < 0.01$ versus H_2O_2-treated cells.

Quercetin (20 μg/ml), served as positive control in this study, significantly inhibited cytotoxicity induced by H_2O_2 treatment. Cynaroside (100 μg/ml) showed protective effect comparable to that of quercetin. Similar results were also found in the following study. These results indicate that cynaroside can protect H9c2 cells from oxidative stress-induced cell injury.

CYNAROSIDE AMELIORATED H_2O_2-INDUCED MORPHOLOGICAL CHANGES IN H9c2 CELLS

Under an inverted microscope (Fig. 3), the cells of the control group appeared to have complete packing membranes, normal spindle shapes, and round nuclei. In contrast, incomplete cellular membranes, cellular swelling, and vacuole degeneration were seen in the H_2O_2-induced groups. Cynaroside pretreatment caused a dose-dependent amelioration of the morphological changes caused by H_2O_2.

CYNAROSIDE REDUCED LIPID PEROXIDATION AND ENHANCED ANTI-OXIDANT ENZYME ACTIVITY IN H_2O_2-TREATED H9c2 CELLS

LDH, which leaks from cells after plasma membrane disruption, can be used as an indicator of cell injury. Membrane lipid oxidation is one of the primary events in oxidative damage, which can be assessed by its degradation product MDA [Mahady, 2002; Yang et al., 2008]. Treatment of H9c2 cells with 150 μM H_2O_2 caused a significant increase in LDH release and intracellular MDA levels, whereas preincubation with 100 and 50 μg/ml cynaroside markedly ameliorated the increase in LDH release and intracellular MDA levels (Table I). In addition, the activities of some endogenous anti-oxidative enzymes, such as SOD, CAT, and GSH-Px activity in the H_2O_2-treated cells were decreased compared with the control, whereas pretreatment with cynaroside effectively ameliorated the decreased activity of SOD, CAT, and GSH-Px. These data suggest that cynaroside reduces oxidative injury by enhancing the endogenous anti-oxidant capacity.

CYNAROSIDE DECREASED H_2O_2-INDUCED APOPTOSIS IN H9c2 CELLS

Hoechst 33342 staining was used to determine the effects of cynaroside on apoptosis induced by H_2O_2 in H9c2 cells. As shown in Figure 4A, using a fluorescence microscope, oval-shaped nuclei with homogeneous fluorescence intensity were observed in the normal cells, and heterogeneous intensity and chromatin condensation were observed in the nuclei of the H_2O_2-induced of H9c2 cells. Pretreatment with cynaroside alleviated significantly the morphological changes caused by H_2O_2 treatment. As shown in Figure 4B, the percentage of apoptotic cells was 12.7% in control group, and 45.2% in H_2O_2-treated cells. There were significantly fewer apoptotic cells 39.3%, 23.7%, and 20.3% in the 25, 50, and 100 μg/ml cynaroside pretreatment groups, respectively. The anti-apoptotic effect of cynaroside was further confirmed by the flow cytometry analysis of the samples stained with FITC-Annexin V/PI (Fig. 4C). As shown in Figure 4D, the apoptosis rate in the H_2O_2 model group was 29.2%, whereas it was reduced to 20.7% and 11.5% with 50 and 100 μg/ml cynaroside, respectively.

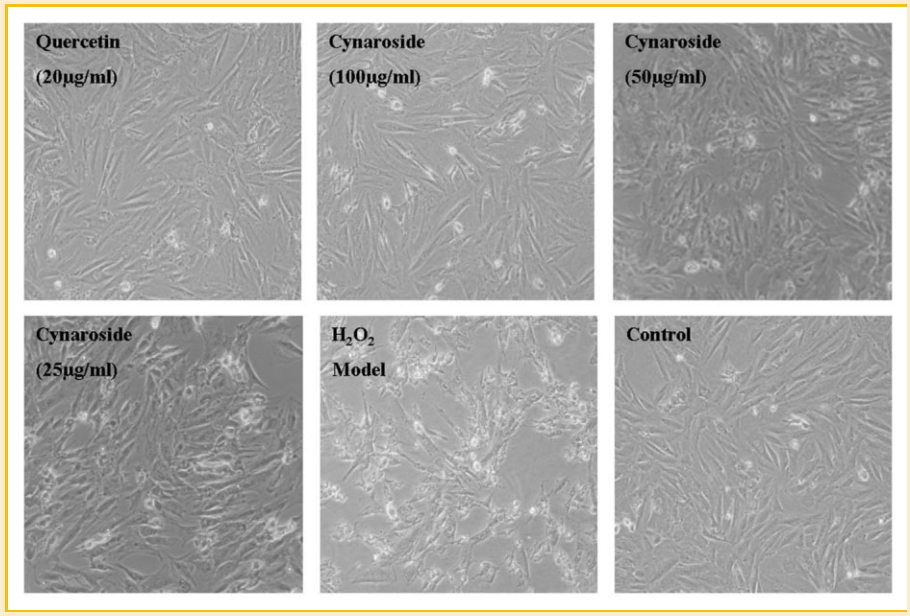

Fig. 3. Effects of cynaroside on morphological changes in H_2O_2-treated H9c2 cells. Cell morphology was observed after 6 h of H_2O_2 exposure. The representative images are from three independent experiments. H_2O_2 resulted in significant abnormal morphology, whereas pretreatment with cynaroside caused a dose-dependent recovery from the H_2O_2-induced morphological changes (light microscopy, original magnification 200×).

CYNAROSIDE INHIBITED INTRACELLULAR ROS GENERATION

Production of ROS was monitored using flow cytometry. As shown in Figure 5A, the intracellular ROS levels were increased after H_2O_2 treatment for 6 h, as demonstrated by the shift in fluorescence from left to the right. Statistical analysis of results showed that the percentage of cells with increased ROS production was 46.8% in H_2O_2-treated group, which was decreased by cynaroside pretreatment down to 42.0%, 22.0%, and 16.1%, respectively, for 25, 50, and 100 μg/ml cynaroside (Fig. 5B). Our preliminary study showed that cynaroside alone could not affect intracellular ROS level (data not shown). Results showed that cynaroside pretreatment significantly decreased the generation of intracellular ROS in a dose-dependent manner.

CYNAROSIDE RESTORED $\Delta\Psi_m$ FOLLOWING INCUBATION WITH H_2O_2

Excessive ROS production led to a collapse of $\Delta\Psi_m$, triggering intrinsic cell death through the mitochondria-mediated pathway [Ott et al., 2007]. JC-1 exhibited a potential-dependent accumulation in the mitochondria and the mitochondrial depolarization was indicated by a decrease in the red/green fluorescence intensity ratio. As shown in Figure 6A, H_2O_2-induced oxidative stress caused a dissipation of $\Delta\Psi_m$, signified by the shift of fluorescence from right upper to lower right in the panel. Cynaroside significantly alleviated H_2O_2-induced loss of $\Delta\Psi_m$ (Fig. 6B). In normal control group, the percentage of cells with depolarized mitochondria was 14.9%, while it was increased up to 46.3% in H_2O_2-treated cells. Cynaroside significantly decreased the percentage to 22.9% and 28.4% at 100 and 50 μg/ml, respectively. These results demonstrate that the anti-apoptotic effect of cynaroside was probably due to the stabilization of mitochondrial dysfunction.

CYNAROSIDE INHIBITED CASPASE-3 ACTIVATION AND THE ACTIVITY OF CASPASE-8 AND CASPASE-9

The caspase enzymes regulate many of the events leading to the cellular and biochemical changes associated with apoptosis [Ryter et al., 2007]. Flow cytometry analysis, as shown in Figure 7A, revealed that the ratio of activated caspase-3 increased significantly in the H_2O_2-treatment group. However, lower levels of activated caspase-3 in the cynaroside pretreatment group were

TABLE I. Effects of Cynaroside on Lipid Peroxidation and Anti-Oxidant Enzyme Activity (Means ± SD, n = 3)

Group	LDH (U/L)	MDA (nmol/mg protein)	SOD (U/mg protein)	GSH-Px (U/mg protein)	CAT (U/mg protein)
Control	181.83 ± 21.60	1.10 ± 0.17	84.88 ± 10.12	3.50 ± 0.46	34.26 ± 4.47
H_2O_2	1870.1 ± 73.4$^{\#\#}$	3.49 ± 0.53$^{\#\#}$	30.89 ± 3.89$^{\#\#}$	1.40 ± 0.29$^{\#\#}$	13.35 ± 0.38$^{\#\#}$
Cyn (25 μg/ml)	1298.73 ± 89.32**	3.25 ± 0.97	29.39 ± 2.19	1.38 ± 0.13	13.52 ± 1.25
Cyn (50 μg/ml)	753.17 ± 58.64**	1.64 ± 0.28**	51.07 ± 1.99**	1.70 ± 0.07	18.35 ± 0.88*
Cyn (100 μg/ml)	467.50 ± 39.2**	1.46 ± 0.15**	69.35 ± 3.11**	2.31 ± 0.10**	22.65 ± 1.02**
Que (20 μg/ml)	493.5 ± 15.71**	1.35 ± 0.25**	71.76 ± 1.23**	3.03 ± 0.36**	29.65 ± 3.55**

$^{\#\#}P < 0.01$ versus control and $^{*}P < 0.05$, $^{**}P < 0.01$ versus H_2O_2.

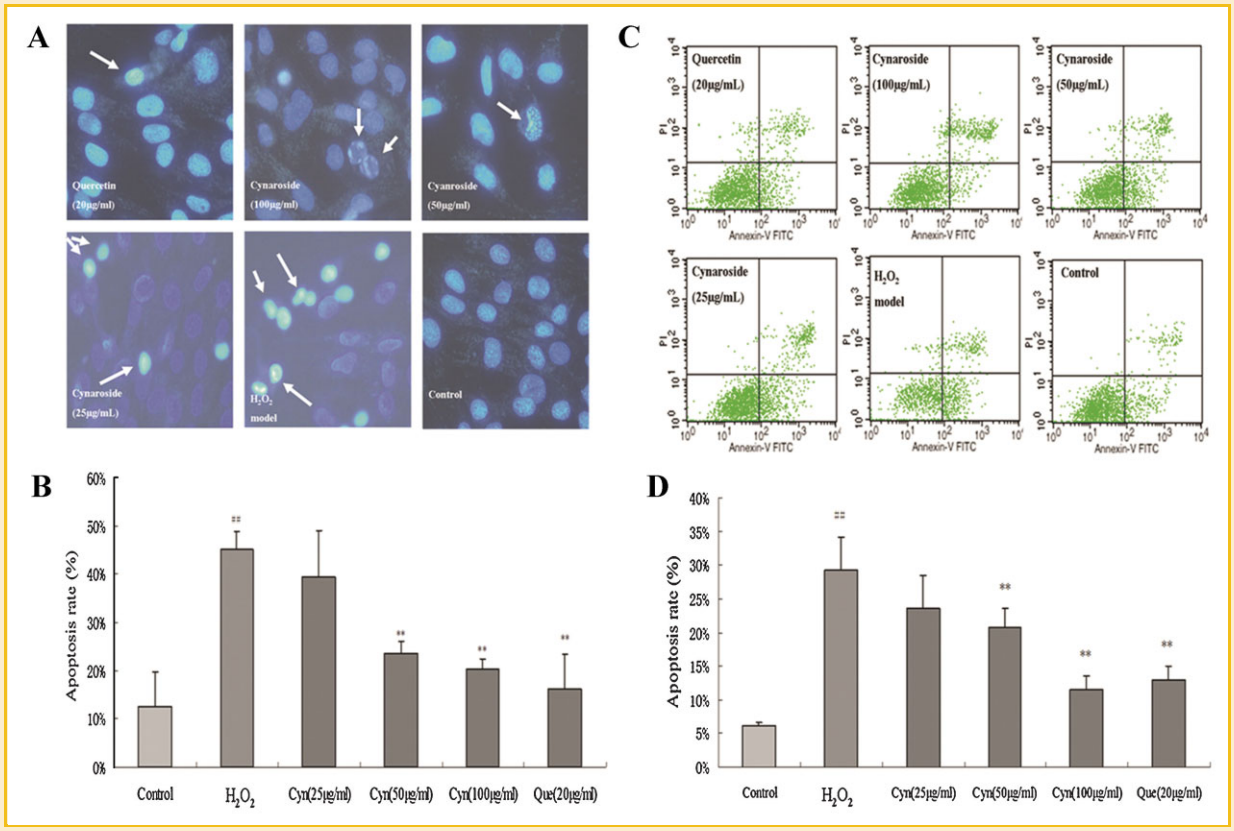

Fig. 4. Effects of cynaroside on H_2O_2-induced apoptosis in H9c2 cells. The cells were pretreated with different concentrations of cynaroside or quercetin (20 μg/ml) for 4 h followed by H_2O_2 (150 μM) treatment for 6 h and stained with Hoechst 33342. Then, the cells were visualized under fluorescent microscope. Each photograph is representative of three independent observations. The apoptotic cells were identified as those with nuclei exhibiting brightly stained condensed chromatin (Hoechst-positive cells) (A). The apoptosis rate was determined by calculating the percentage of Hoechst-positive cells over the total number of cells. Arrowheads in the pictures indicate the nuclei of the apoptotic cells (Hoechst-positive cells) (B). Flow cytometry analysis of the Annexin V-FITC/PI staining in H9c2 cells (C) and statistical analysis of the flow cytometry data (D). All data are presented as means ± SD from three independent experiments. $^{\#\#}P < 0.01$ versus control; $^{*}P < 0.05$ versus H_2O_2-treated cells; $^{**}P < 0.01$ versus H_2O_2-treated cells.

observed. Compared with the control, caspase-8 activity increased by 3.67-fold after 150 μM H_2O_2 treatment for 6 h. It was inhibited significantly by the cynaroside preincubation, dropping to 1.43- and 1.11-fold, respectively, with 50 and 100 μg/ml cynaroside (Fig. 7B). For the caspase-9 activity, the cells were treated with 150 μM H_2O_2 for the indicated periods after 4 h pretreatment with 100 μg/ml cynaroside. Then, the catalytic activity was assessed using the fluorogenic biosubstrate, LEHD-AFC. The caspase-9 activity increased significantly at 1 h, and reached a peak level upon 4 h of H_2O_2 treatment. Pretreatment with cynaroside significantly suppressed the catalytic activation of caspase-9 (Fig. 7C).

CYNAROSIDE MODULATED APOPTOSIS-RELATED PROTEIN EXPRESSION IN H_2O_2-TREATED H9c2 CELLS

The effects of cynaroside on the expression of apoptosis-related proteins were examined using Western blot analysis. The H_2O_2-induced apoptosis is accompanied by a decreased expression of anti-apoptotic protein Bcl-2, but an increased pro-apoptotic protein Bax expression, which are two well-known proteins in the Bcl-2 family that regulate mitochondrial outer membrane permeability [Ryter et al., 2007]. Pretreatment with cynaroside prevented the decrease in the Bcl-2 expression whereas it suppressed the increase in Bax expression, therefore reduced the release of apoptogenic factors (cytochrome *c* and Smac/Diablo) as shown by the increase expression in the cytosol and a decrease in the mitochondrial fraction (Fig. 8). Cynaroside also showed an inhibitory effect on H_2O_2-induced elevation of Apaf-1 expression. H_2O_2 caused an increase in the expression of the transcription factor p53, known to lead the expression of proteins that prevent cell division and cause apoptosis. In the cynaroside treatment group, the upregulated expression of p53 was inhibited. Treatment of H9c2 cells with 150 μM H_2O_2 resulted in the activation of JNK. However, the activation of JNK was clearly reduced by the cynaroside pretreatment.

DISCUSSION

Considerable evidence supports that apoptosis plays a crucial role in the pathogenesis of various cardiovascular diseases due to the loss of terminally differentiated cardiomyocytes [Bae et al., 2008; Lee and Gustafsson, 2009; Kim and Kang, 2010]. Oxidative stress mediated by ROS is an essential mechanism causing cardiac myocyte apoptosis in pathological conditions such as ischemia/reperfusion

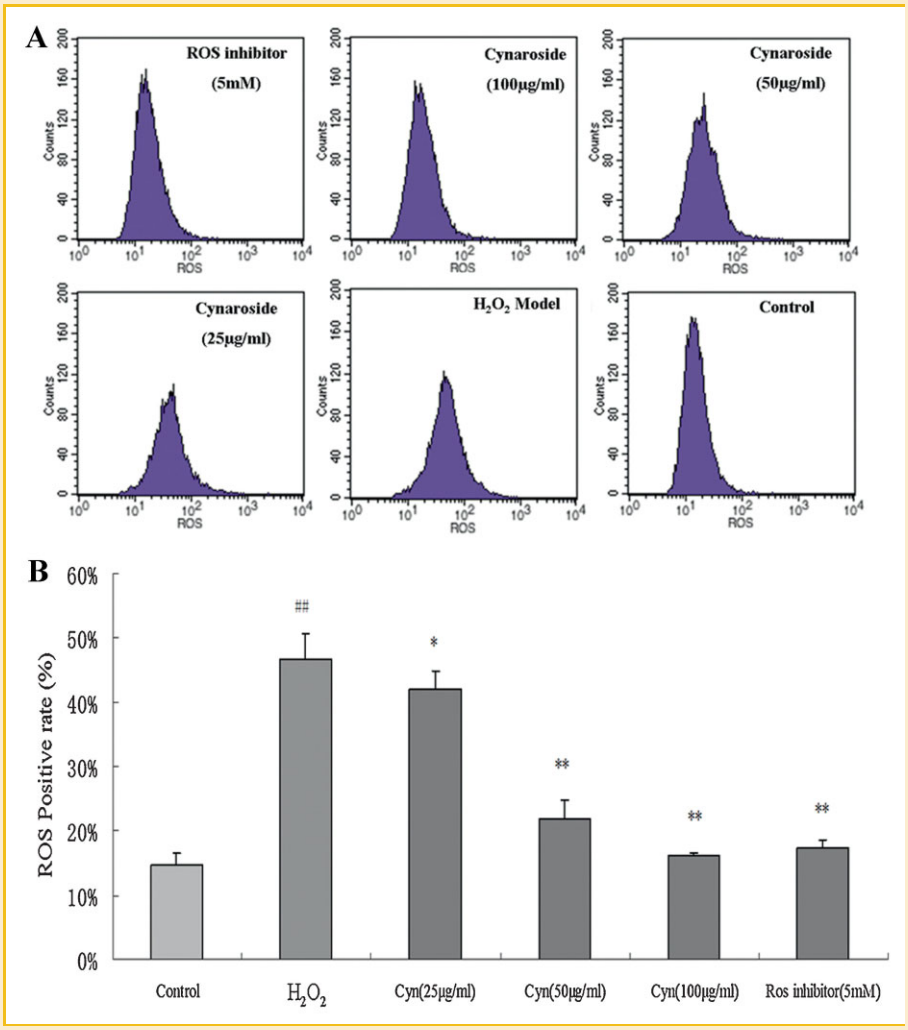

Fig. 5. Effects of cynaroside on the intracellular generation of ROS. The cells were treated with 150 μM H_2O_2 in the absence or presence of cynaroside for 6 h. Then, the cells were incubated with the fluorescent dye for 30 min, and the fluorescence intensity was analyzed by flow cytometry. A: Flow cytometry analysis of the intracellular ROS. B: Statistical analysis of the flow cytometry data. Data are presented as means ± SD from three independent experiments. $^{\#\#}P < 0.01$ versus control; $^{*}P < 0.05$ versus H_2O_2-treated cells; $^{**}P < 0.01$ versus H_2O_2-treated cells.

injury, myocardium remodeling after myocardial infarction and heart failure, etc. [Cheng et al., 2009; Han et al., 2009; Luo et al., 2009; Mishra et al., 2010]. Therefore, inhibition of oxidative stress-induced cardiomyocyte apoptosis process yields critical intervention strategies to manage those diseases. In this study, cynaroside markedly suppressed the increase in intracellular ROS levels caused by H_2O_2 treatment and reduced H_2O_2-induced apoptotic cell death in a dose-dependent manner. These results indicate that cynaroside exerts protects against H_2O_2-induced H9c2 cell apoptosis.

Oxidative stress is generally defined as an imbalance between ROS production and elimination that results in over accumulation of intracellular ROS, which can initiate apoptosis [Ott et al., 2007]. To defend against possible deleterious effects of ROS, cells maintain an endogenous anti-oxidative capacity consisting of SOD, CAT, and GSH-Px enzyme systems that remove ROS by metabolic conversion. SOD catalyzes the conversion of O_2^- to H_2O_2, which is then converted to water and O_2 by CAT, whereas GSH-Px maintains sulfhydryl buffering capacity [Ryter et al., 2007]. These enzymes protect against various forms of oxidative cardiovascular injuries [Han et al., 2008]. In our study, the enzymes activities of SOD, GSH-Px, and CAT in the H_2O_2 group were significantly decreased, causing an inability to eliminate the excessive amount of ROS promptly. This was consistent with our results that ROS concentration was significantly increased after H_2O_2 treatment. However, cynaroside pretreatment significantly increased the activities of SOD, CAT, and GSH-Px and decreased intracellular ROS levels. In vivo studies [Edenharder and Grunhage, 2003] showed that cynaroside exerted anti-oxidative effect by directly scavenging free radicals, while our results showed that it might also be associated with its enhancing endogenous anti-oxidative activities, thereby inhibiting the abnormal accumulation of intracellular ROS in the cells.

Apoptosis may be initiated either by the intrinsic (mitochondrial) or by the extrinsic (death receptor-dependent) pathways [Ryter et al., 2007]. Caspases are a family of aspartate-specific cysteine proteases

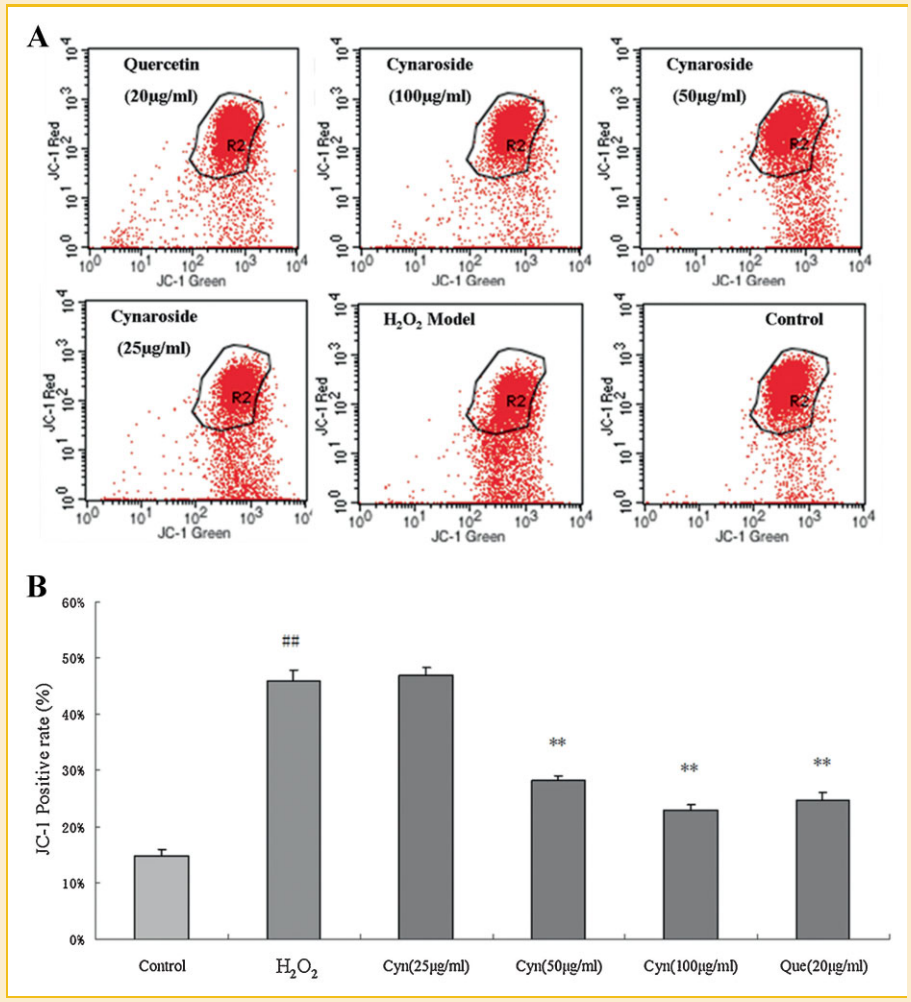

Fig. 6. Flow cytometry analysis of mitochondrial membrane potential by JC-1 staining in H9c2 cells. The cells were pretreated with cynaroside for 4 h followed by incubation for 6 h with 150 μM H_2O_2. Then, the cells were stained with 2 μM JC-1 for 30 min and analyzed by flow cytometry. Data are presented as means ± SD from three independent experiments. $^{\#\#}P < 0.01$ versus control; $^{*}P < 0.05$ versus H_2O_2-treated cells; $^{**}P < 0.01$ versus H_2O_2-treated cells.

that play key roles in regulating the two pathways of apoptosis induced by different stimuli, including oxidative stress [Earnshaw et al., 1999]. Caspase-3 is the key executioner of apoptosis, regulating factors involved in DNA degradation, chromatin condensation, and nuclear fragmentation. Caspase-3 was activated by H_2O_2 treatment and cynaroside pretreatment dose-dependently inhibited the activation, indicating that the protective effect of cynaroside is involved in regulating the caspases cascade. Researches have shown that the activation of caspase-3 could be initiated by upstream protease, either by caspase-9 in intrinsic apoptosis pathways involving mitochondrial dysfunction or by caspase-8 in extrinsic apoptosis pathways involving death receptors [Ryter et al., 2007]. Previous studies [Park et al., 2003] have reported that H_2O_2 treatment increased caspase-9 activity in H9c2 cells, indicating that the mitochondrial pathway played an important role in H_2O_2-induced apoptosis in H9c2 cells. Interestingly, our results showed that caspase-8 activity was also significantly increased in this model. This further confirmed that the death receptor pathway was also involved in H_2O_2-induced H9c2 cell apoptosis. One hundred and 50 μg/ml cynaroside pretreatment inhibited the increase in caspase-8 and caspase-9 activity, suggesting that the anti-apoptotic effects of cynaroside may be associated with suppressing the activation of both the extrinsic and intrinsic pathway of apoptosis.

The mitochondria play a central role in apoptosis [Ott et al., 2007; Lee and Gustafsson, 2009], integrating apoptotic signals from both the mitochondrial and death receptor pathways. Mitochondrial membrane permeabilization is the rate-limiting manifestation of mitochondrial cell death. The disruption of the mitochondrial transmembrane potential $\Delta\psi_m$ leads to the release of pro-apoptotic molecules such as cytochrome *c* and Smac/Diablo from the intermembrane space to the cytoplasm, where cytochrome *c* forms apoptosome with Apaf-1 and caspase-9, promoting caspase-9 activation, whereas Smac/Diablo indirectly activates caspase by binding to inhibitor of apoptosis proteins (IAPs) and antagonizing their inhibitory effect on caspase activation [Sussman, 2009]. Consistent with previous reports [Shan et al., 2008], H_2O_2-induced oxidative stress increased ROS levels in the H9c2 cells, and

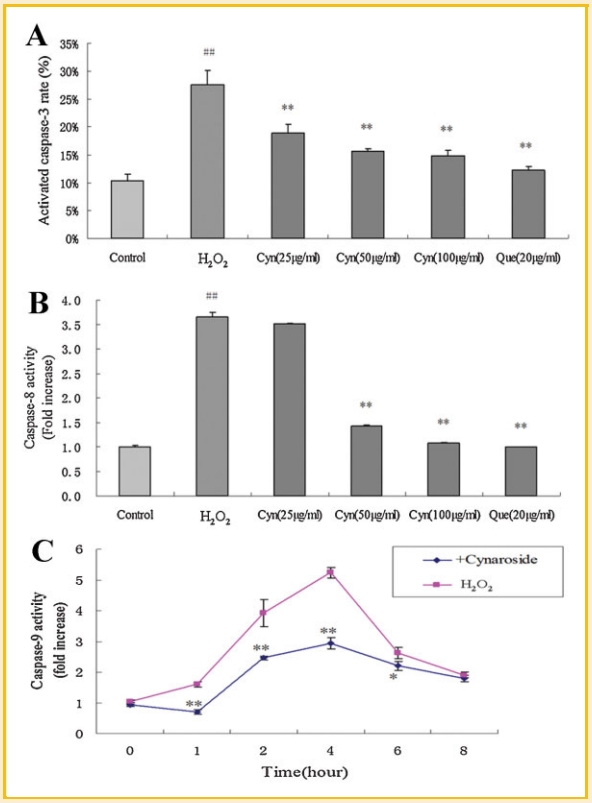

Fig. 7. Effects of cynaroside pretreatment on caspases activities. The cells were pretreated with cynaroside for 4 h followed by 6 h treatment of 150 μM H_2O_2. Flow cytometric analysis of activated caspase-3 (A). Caspase-8 activity was measured by fluorometric assay (B, expressed as fold-increases compared with that of control). Caspase-9 activity was measured by fluorometric assay (C, expressed as fold-increases compared with that of control). The cells were pretreated with 100 μg/ml cynaroside followed by H_2O_2 treatment for the indicated periods. Results are presented as means ± SD from three independent experiments. $^{\#\#}P < 0.01$ versus control $^{*}P < 0.05$ and $^{**}P < 0.01$ versus H_2O_2-treated cells.

subsequently caused mitochondrial depolarization and dissipation of $\Delta\psi_m$. One hundred and 50 μg/ml cynaroside stabilized the H_2O_2-induced mitochondrial dysfunction, as shown by the preservation of mitochondrial potential, therefore reduced the release of pro-apoptotic molecules from mitochondria. In addition, cynaroside pretreatment inhibited the increased expression of Apaf-1, thus prevented the formation of apoptosome and the subsequent activation of caspase-9. Furthermore, our results showed that cynaroside modulated the protein expression of the Bcl-2 family of proteins. The Bcl-2 proteins are the major regulators of mitochondrial permeabilization, which includes pro-apoptotic (e.g., Bax and Bak) and anti-apoptotic (e.g., Bcl-2 and Bcl-xL) members. Bax oligomerization at the outer mitochondrial membrane causes transmembrane pore formation, leading to the release of pro-apoptotic molecules into the cytoplasm, whereas Bcl-2 forms heterodimers with a variety of pro-apoptotic proteins, thereby prevent Bax oligomerization [Kuwana and Newmeyer, 2003]. The cynaroside pretreatment increased the expression of Bcl-2, as it decreased the expression of pro-apoptotic Bax. Therefore, cynaroside might exert protective effects by maintaining mitochondrial function and modulating the balance between anti-apoptotic protein Bcl-2 and pro-apoptotic protein Bax, thus inhibiting the release of pro-apoptotic molecules from the mitochondrial intermembrane space into the cytoplasm.

Interestingly in our study, high concentration of cynaroside (100 and 50 μg/ml) and low concentration of cynaroside (25 μg/ml) exhibited discrepancy in mechanism of protection on H_2O_2-induced apoptosis. One hundred and 50 μg/ml cynaroside inhibited the activation of both caspase-8 and caspase-9, while cynaroside at 25 μg/ml showed no effects on caspase-8 activities, indicating that its protective effects were not related to the inhibition of extrinsic pathway activation. Moreover, results showed that 25 μg/ml cynaroside inhibited caspase-9 activation (data not shown); however, it showed no effects on the dissipation of mitochondrial potential and the release of cytochrome *c*. Several recent studies suggested that caspase-9 activation could be independent of cytochrome *c* release [Hao et al., 2005; Yu et al., 2006; Zuo et al., 2009]. Zuo et al. found that ROS could oxidatively modify caspase-9, thus facilitating the interaction of caspase-9 and Apaf-1 and promoting subsequent cleavage and activation caspase-9 in a mitochondria-free system. In our study, since 25 μg/ml cynaroside showed no effects on mitochondrial potential, it might achieve its protective effects by reducing intracellular ROS level, therefore directly inhibiting the oxidative modification of caspase-9 and subsequent activation of caspase-9. Therefore, high concentration of cynaroside protected H_2O_2-induced apoptosis through inhibiting the activation of both intrinsic pathway and extrinsic pathway, while low concentration of cynaroside achieved its effectiveness by reducing intracellular ROS, thus inhibiting oxidative modification and activation of caspase-9.

We evaluated the role of the JNK and P53 pathways to thoroughly examine the mechanisms by which cynaroside modulates H_2O_2-induced apoptosis. Mitogen-activated protein kinases (MAPKs) belong to an evolutionary conserved and ubiquitous signal transduction superfamily of ser/thr protein kinases that regulate apoptosis and other cellular programs. Activation of the MAPK pathways (i.e., JNK, ERK1/2, and p38 MAPK) is a feature of oxidant-induced apoptosis [Ryter et al., 2007]. Although the role of the JNK pathway in apoptosis remains controversial because both pro-apoptotic and anti-apoptotic effects have been observed to be dependent on cell type and apoptotic stimuli [Shen and Liu, 2006], JNK activation is important in the H_2O_2-induced apoptotic cell death in H9c2 cells [Turner et al., 1998; Hong et al., 2001; Pechtelidou et al., 2008]. In accordance with previous findings, our results showed that H_2O_2 treatment of H9c2 cells increased phosphor-JNK expression [Duplain, 2006; Yang et al., 2008]. JNK activation could directly inactivate anti-apoptotic protein Bcl-2 by phosphorylation and increase cytochrome *c* release [Yamamoto et al., 1999; Tournier et al., 2000]. Cynaroside pretreatment alleviated the H_2O_2-induced elevation of phosphor-JNK expression, thus regulating the release of pro-apoptotic factors from the mitochondria. The increased intracellular ROS level causes DNA damage, which activates the transcriptional factor P53, a DNA-binding transcription factor that up-regulates growth arrest and apoptosis-related genes in response to stress signals. In the present study, H_2O_2-induced apoptosis was

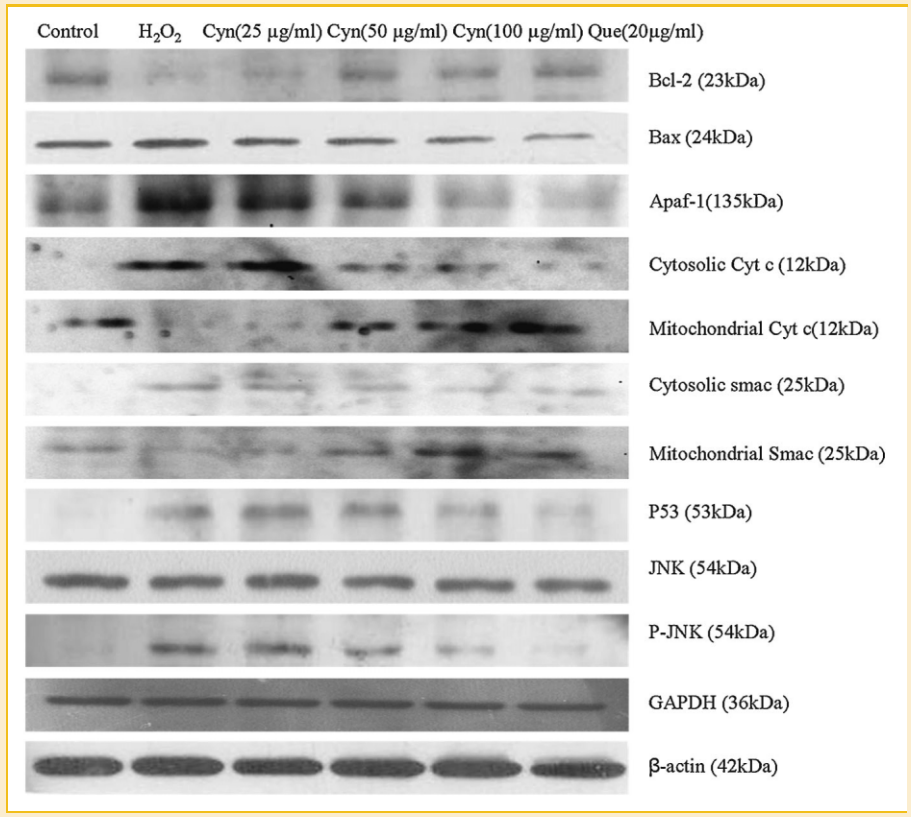

Fig. 8. Effects of cynaroside pretreatment on apoptotic-related protein expression. The cells were pretreated with cynaroside for 4 h followed by 6 h treatment with 150 μM H_2O_2. Expression of apoptotic-related proteins was analyzed by Western blotting with corresponding antibodies. Data are representative of three different experiments.

accompanied by an increased expression of P53. The elevated expression in P53 may subsequently trigger the expression of pro-apoptotic protein Bax, which enhances mitochondrial permeability and induces pro-apoptotic factors such as cytochrome *c* release, as well as the subsequent activation of the caspase cascade [Liu et al., 2008; Oyama et al., 2009; Sheng et al., 2010]. However, pretreatment with cynaroside could inhibit the expression of P53, thereby inhibiting H_2O_2-induced apoptosis.

In conclusion, the results of this study demonstrated that cynaroside protected H9c2 cells against H_2O_2-induced apoptosis by decreasing ROS generation and inhibiting caspase activation in both the mitochondrial and death receptor pathways. Furthermore, cynaroside maintained mitochondrial function by regulating Bcl-2 protein expression, as well as JNK and P53 expression. Although cynaroside is a promising agent for the treatment of H_2O_2-induced apoptosis, further investigations are necessary to explore the underlying mechanisms of cynaroside cytoprotection against oxidative stress-induced cardiovascular diseases.

ACKNOWLEDGMENTS

The work was supported by grants from Key Projects in the National Science & Technology Pillar Program (No. 2008BAI51B02) and Major Scientific and Technological Special Project for ''Significant New Drugs Formulation ''(No. 2009ZX09301-003).

REFERENCES

Bae S, Yalamarti B, Kang PM. 2008. Role of caspase-independent apoptosis in cardiovascular diseases. Front Biosci 13:2495–2503.

Bent S. 2008. Herbal medicine in the United States: Review of efficacy, safety, and regulation: Grand rounds at University of California, San Francisco Medical Center. J Gen Intern Med 23:854–859.

Brown JE, Rice-Evans CA. 1998. Luteolin-rich artichoke extract protects low density lipoprotein from oxidation in vitro. Free Radic Res 29:247–255.

Cheng Y, Liu X, Zhang S, Lin Y, Yang J, Zhang C. 2009. MicroRNA-21 protects against the H(2)O(2)-induced injury on cardiac myocytes via its target gene PDCD4. J Mol Cell Cardiol 47:5–14.

Duplain H. 2006. Salvage of ischemic myocardium: A focus on JNK. Adv Exp Med Biol 588:157–164.

Earnshaw WC, Martins LM, Kaufmann SH. 1999. Mammalian caspases: Structure, activation, substrates, and functions during apoptosis. Annu Rev Biochem 68:383–424.

Edenharder R, Grunhage D. 2003. Free radical scavenging abilities of flavonoids as mechanism of protection against mutagenicity induced by tert-butyl hydroperoxide or cumene hydroperoxide in Salmonella typhimurium TA102. Mutat Res 540:1–18.

Fu J, Huang H, Liu J, Pi R, Chen J, Liu P. 2007. Tanshinone IIA protects cardiac myocytes against oxidative stress-triggered damage and apoptosis. Eur J Pharmacol 568:213–221.

Gottlieb RA, Burleson KO, Kloner RA, Babior BM, Engler RL. 1994. Reperfusion injury induces apoptosis in rabbit cardiomyocytes. J Clin Invest 94:1621–1628.

Han X, Pan J, Ren D, Cheng Y, Fan P, Lou H. 2008. Naringenin-7-O-glucoside protects against doxorubicin-induced toxicity in H9c2 cardiomyocytes by induction of endogenous antioxidant enzymes. Food Chem Toxicol 46:3140–3146.

Han SY, Li HX, Ma X, Zhang K, Ma ZZ, Tu PF. 2009. Protective effects of purified safflower extract on myocardial ischemia in vivo and in vitro. Phytomedicine 16:694–702.

Hao Z, Duncan GS, Chang CC, Elia A, Fang M, Wakeham A, Okada H, Calzascia T, Jang Y, You-Ten A, Yeh WC, Ohashi P, Wang X, Mak TW. 2005. Specific ablation of the apoptotic functions of cytochrome C reveals a differential requirement for cytochrome C and Apaf-1 in apoptosis. Cell 121:579–591.

Hescheler J, Meyer R, Plant S, Krautwurst D, Rosenthal W, Schultz G. 1991. Morphological, biochemical, and electrophysiological characterization of a clonal cell (H9c2) line from rat heart. Circ Res 69:1476–1486.

Hong F, Kwon SJ, Jhun BS, Kim SS, Ha J, Kim SJ, Sohn NW, Kang C, Kang I. 2001. Insulin-like growth factor-1 protects H9c2 cardiac myoblasts from oxidative stress-induced apoptosis via phosphatidylinositol 3-kinase and extracellular signal-regulated kinase pathways. Life Sci 68:1095–1105.

Kang PM, Izumo S. 2000. Apoptosis and heart failure: A critical review of the literature. Circ Res 86:1107–1113.

Khor GL. 2001. Cardiovascular epidemiology in the Asia-Pacific region. Asia Pac J Clin Nutr 10:76–80.

Kim NH, Kang PM. 2010. Apoptosis in cardiovascular diseases: Mechanism and clinical implications. Korean Circ J 40:299–305.

Kimes BW, Brandt BL. 1976. Properties of a clonal muscle cell line from rat heart. Exp Cell Res 98:367–381.

Kuwana T, Newmeyer DD. 2003. Bcl-2-family proteins and the role of mitochondria in apoptosis. Curr Opin Cell Biol 15:691–699.

Lee Y, Gustafsson AB. 2009. Role of apoptosis in cardiovascular disease. Apoptosis 14:536–548.

Liu J, Mao W, Ding B, Liang CS. 2008. ERKs/p53 signal transduction pathway is involved in doxorubicin-induced apoptosis in H9c2cells and cardiomyocytes. Am J Physiol Heart Circ Physiol 295:H1956–H1965.

Luo X, Cai H, Ni J, Bhindi R, Lowe HC, Chesterman CN, Khachigian LM. 2009. c-Jun DNAzymes inhibit myocardial inflammation, ROS generation, infarct size, and improve cardiac function after ischemia-reperfusion injury. Arterioscler Thromb Vasc Biol 29:1836–1842.

Mahady GB. 2002. *Ginkgo biloba* for the prevention and treatment of cardiovascular disease: A review of the literature. J Cardiovasc Nurs 16: 21–32.

Mishra PK, Tyagi N, Sen U, Givvimani S, Tyagi SC. 2010. H2S ameliorates oxidative and proteolytic stresses and protects the heart against adverse remodeling in chronic heart failure. Am J Physiol Heart Circ Physiol 298:H451–H456.

Mojzisova G, Sarissky M, Mirossay L, Martinka P, Mojzis J. 2009. Effect of flavonoids on daunorubicin-induced toxicity in H9c2 Cardiomyoblasts. Phytother Res 23:136–139.

Ng TB. 2006. Pharmacological activity of sanchi ginseng (*Panax notoginseng*). J Pharm Pharmacol 58:1007–1019.

Ott M, Gogvadze V, Orrenius S, Zhivotovsky B. 2007. Mitochondria, oxidative stress and cell death. Apoptosis 12:913–922.

Oyama K, Takahashi K, Sakurai K. 2009. Cardiomyocyte H9c2 cells exhibit differential sensitivity to intracellular reactive oxygen species generation with regard to their hypertrophic vs death responses to exogenously added hydrogen peroxide. J Clin Biochem Nutr 45:361–369.

Park C, So HS, Shin CH, Baek SH, Moon BS, Shin SH, Lee HS, Lee DW, Park R. 2003. Quercetin protects the hydrogen peroxide-induced apoptosis via inhibition of mitochondrial dysfunction in H9c2 cardiomyoblast cells. Biochem Pharmacol 66:1287–1295.

Pechtelidou A, Beis I, Gaitanaki C. 2008. Transient and sustained oxidative stress differentially activate the JNK1/2 pathway and apoptotic phenotype in H9c2cells. Mol Cell Biochem 309:177–189.

Pryor WA, Houk KN, Foote CS, Fukuto JM, Ignarro LJ, Squadrito GL, Davies KJ. 2006. Free radical biology and medicine: It's a gas, man. Am J Physiol Regul Integr Comp Physiol 291:R491–R511.

Rump AF, Schussler M, Acar D, Cordes A, Theisohn M, Rosen R, Klaus W, Fricke U. 1994. Functional and antiischemic effects of luteolin-7-glucoside in isolated rabbit hearts. Gen Pharmacol 25:1137–1142.

Ryter SW, Kim HP, Hoetzel A, Park JW, Nakahira K, Wang X, Choi AM. 2007. Mechanisms of cell death in oxidative stress. Antioxid Redox Signal 9:49–89.

Shan P, Pu J, Yuan A, Shen L, Chai D, He B. 2008. RXR agonists inhibit oxidative stress-induced apoptosis in H9c2 rat ventricular cells. Biochem Biophys Res Commun 375:628–633.

Shen HM, Liu ZG. 2006. JNK signaling pathway is a key modulator in cell death mediated by reactive oxygen and nitrogen species. Free Radic Biol Med 40:928–939.

Sheng R, Gu ZL, Xie ML, Zhou WX, Guo CY. 2010. Epigallocatechin gallate protects H9c2 cardiomyoblasts against hydrogen dioxides-induced apoptosis and telomere attrition. Eur J Pharmacol 641:199–206.

Smith D. 2000. Cardiovascular disease: A historic perspective. Jpn J Vet Res 48:147–166.

Sussman MA. 2009. Mitochondrial integrity: Preservation through Akt/Pim-1 kinase signaling in the cardiomyocyte. Expert Rev Cardiovasc Ther 7:929–938.

Tournier C, Hess P, Yang DD, Xu J, Turner TK, Nimnual A, Bar-Sagi D, Jones SN, Flavell RA, Davis RJ. 2000. Requirement of JNK for stress-induced activation of the cytochrome c-mediated death pathway. Science 288: 870–874.

Turner NA, Xia F, Azhar G, Zhang X, Liu L, Wei JY. 1998. Oxidative stress induces DNA fragmentation and caspase activation via the c-Jun NH2-terminal kinase pathway in H9c2 cardiac muscle cells. J Mol Cell Cardiol 30:1789–1801.

Wu ML, Tsai KL, Wang SM, Wu JC, Wang BS, Lee YT. 1996. Mechanism of hydrogen peroxide and hydroxyl free radical-induced intracellular acidification in cultured rat cardiac myoblasts. Circ Res 78:564–572.

Wu MJ, Huang CL, Lian TW, Kou MC, Wang L. 2005. Antioxidant activity of Glossogyne tenuifolia. J Agric Food Chem 53:6305–6312.

Yamamoto K, Ichijo H, Korsmeyer SJ. 1999. BCL-2 is phosphorylated and inactivated by an ASK1/Jun N-terminal protein kinase pathway normally activated at G(2)/M. Mol Cell Biol 19:8469–8478.

Yang R, Liu A, Ma X, Li L, Su D, Liu J. 2008. Sodium tanshinone IIA sulfonate protects cardiomyocytes against oxidative stress-mediated apoptosis through inhibiting JNK activation. J Cardiovasc Pharmacol 51:396–401.

Yu X, Wang L, Acehan D, Wang X, Akey CW. 2006. Three-dimensional structure of a double apoptosome formed by the Drosophila Apaf-1 related killer. J Mol Biol 355:577–589.

Zhang SY, Chen G, Wei PF, Huang XS, Dai Y, Shen YJ, Chen SL, Sun-Chi CA, Xu HX. 2008. The effect of puerarin on serum nitric oxide concentration and myocardial eNOS expression in rats with myocardial infarction. J Asian Nat Prod Res 10:373–381.

Zhou W, Chai H, Lin PH, Lumsden AB, Yao Q, Chen C. 2004. Clinical use and molecular mechanisms of action of extract of *Ginkgo biloba* leaves in cardiovascular diseases. Cardiovasc Drug Rev 22:309–319.

Zuo Y, Xiang B, Yang J, Sun X, Wang Y, Cang H, Yi J. 2009. Oxidative modification of caspase-9 facilitates its activation via disulfide-mediated interaction with Apaf-1. Cell Res 19:449–457.